ORIGINAL ARTICLE

Short packet communication in underlay cognitive network assisted by an intelligent reflecting surface

Pham Ngoc Son[1] | Tran Trung Duy[2] | Pham Viet Tuan[3] | Tan-Phuoc Huynh[4]

[1]Faculty of Electrical and Electronics Engineering, Ho Chi Minh City University of Technology and Education, Ho Chi Minh City, Vietnam

[2]Department of Electrical Engineering, Posts and Telecommunications Institute of Technology, Ho Chi Minh City, Vietnam

[3]Faculty of Physics, University of Education, Hue University, Hue City, Vietnam

[4]School of Computing and Information Technology, Eastern International University (EIU), Binh Duong, Vietnam

Correspondence
Pham Ngoc Son, Faculty of Electrical and Electronics Engineering, Ho Chi Minh City University of Technology and Education, Ho Chi Minh City, Vietnam.
Email: sonpndtvt@hcmute.edu.vn

Funding information
Ho Chi Minh City University of Technology and Education, Vietnam

Abstract

We propose short packet communication in an underlay cognitive radio network assisted by an intelligent reflecting surface (IRS) composed of multiple reconfigurable reflectors. This scheme, called the IRS protocol, operates in only one time slot (TS) using the IRS. The IRS adjusts its phases to give zero received cumulative phase at the secondary destination, thereby enhancing the end-to-end signal-to-noise ratio. The transmitting power of the secondary source is optimized to simultaneously satisfy the multi-interference constraints, hardware limitations, and performance improvement. Simulation and analysis results of the average block error rates (BLERs) show that the performance can be enhanced by installing more reconfigurable reflectors, increasing the blocklength, lowering the number of required primary receivers, or sending fewer information bits. Moreover, the proposed IRS protocol always outperforms underlay relaying protocols using two TSs for data transmission, and achieves the best average BLER at identical transmission distances between the secondary source and secondary destination. The theoretical analyses are confirmed by Monte Carlo simulations.

KEYWORDS

block error rate, intelligent reflecting surface, reconfigurable intelligent surface, short packet communication, underlay cognitive radio

1 | INTRODUCTION

In most conventional wireless systems, encryption and communication between network devices are performed with long packets. However, short packet communication is required for ultra-reliable and low-latency communications in new-generation mobile networks such as 5G and beyond, which support applications of industrial networks and Internet of Things (IoT) networks [1]. Short packet communication uses information messages with finite blocklength to reduce latency. Furthermore, it is used in conventional cooperative networks as well as by intermediate users operating as amplify-and-forward (AF) and decode-and-forward (DF) relaying devices to increase the system performance [2–5]. The authors in Gu and others [2] investigated two-way AF networks for short packet transmission and discovered a three-time-slot transmission protocol that improves the performance under the conditions of heterogeneous links with low latency and data rate requirements. The authors of Gu

and others [3], derived block error rates (BLERs) for full-duplex and half-duplex relaying networks. They showed that full-duplex relaying networks outperform the half-duplex relaying networks for the same transmit powers and BLER requirements. López and others [4] decreased the BLERs and delay in dual-hop DF networks with wireless energy harvesting, whereas Nouri and others [5] maximized the performance of dual-hop DF networks via maximum ratio combining. Other studies [6–11] evaluated the BLER system performance when short packets were sent in different non-orthogonal multiple access (NOMA) networks. Elsewhere, short packet communication has been used for downlinks of direct-transmission NOMA models [6,10,11] and cooperative NOMA models [8]. Marasinghe and others [9] applied a hybrid automatic repeat request with chase combining to allow shorter packet length and Lai and others [7] allocated different packet lengths to limit insecurity. Li and others [12] implemented short packet transmission in multiple-input multiple-output (MIMO) systems. They optimized the transmit power and signal transmission time to maximize the average data rate. In Tran and others [13], a MIMO NOMA system that serves multiple users simultaneously allowed shorter packets than a MIMO orthogonal multiple access system, demonstrating that MIMO NOMA combinations efficiently reduce the transmission delay.

Recently published works [14–19] have focused on short-packet communication cognitive radio networks. Cognitive radio is a spectrum- sharing solution between primary users in primary networks and secondary users in secondary networks, allowing the efficient use of licensed spectra in primary networks. By selecting one of the sharing protocols (interweave, overlay, or underlay), the secondary users can adaptably and knowledgeably exploit the licensed spectra, guaranteeing that the quality of service of the primary networks is within a given threshold [17,20,21].

The intelligent reflecting surface (IRS) or reconfigurable intelligent surface (RIS) has recently emerged in research on intelligently wireless transmission channels [22–24]. The IRS solution can improve the spectral and energy efficiencies at low hardware cost and small energy consumption, which is especially convenient in practical installations such as wall and ceiling mounts. Moreover, an IRS is easily integrated into the existing wireless systems. An IRS contains multiple reflectors that are independently configured to adjust the phases and amplitudes of the incoming signals. This adjustment changes the transmission directions of the reflected signals into the desired directions that strengthen the signal and decline co-channel interferences at the receivers. Because they require no transmit power amplifiers such

as cooperative communication systems or massive MIMO-equipped networks, IRS-based wireless networks can operate in full-duplex mode without amplifying the interferences [22]. Outstanding results in previous works [25–27] showed that IRS-assisted wireless systems for long packet transmission achieve higher performance and consume lower transmit power than cooperative communication schemes using relays.

1.1 | Related work and motivation

Chen and others [14] used short packet communications and maximal ratio transmission to meet the low-latency and security requirements of cognitive IoT with two transceiver pairs of primary and secondary nodes and a passive eavesdropper. They derived the secrecy throughput under secrecy constraints and the decoding error probability and discussed the impacts of blocklength on transmission delay and secrecy performance. Later, Chen and others expanded their previous security works to cognitive relaying networks [15,16]. The relay design in previous works [15,16] exploits the maximum ratio combining/zero forcing beamforming scheme to guarantee the secrecy performance of dual-hop short-packet communications. In the underlay cognitive relaying network of Ho and others [17], secondary-source and secondary-energy-harvesting relays send short packets to a secondary destination under interference constraints. The relay can be selected to improve the BLER performance. Hu and others [18] considered short-packet communications in spectrum-sharing networks assisted by an unmanned aerial vehicle (UAV). Because the UAV has a limited battery capacity, Hu and others [18] designed the packet error rate, sensing duration, normalized sensing threshold, and transmit power of the UAV to maximize the energy efficiency under the protection constraints at the primary receivers. Vu and others [19] studied a general approach for short-packet communications in wireless-powered cognitive NOMA IoT networks with imperfect channel state information (CSI) and successive interference cancelation. They aimed to improve the spectrum utilization, sustainability, and latency by exploring the performance parameters (average BLER, goodput, energy efficiency, latency, and reliability). Their proposed protocol lowers the latency and improves the reliability from those of the benchmark scheme (long packet communications created in the same model settings). However, previous works [14–19] have ignored the emerging IRS.

Recently, the IRS solution has been considered in cognitive radio networks [28–31]. Xu and others [29] applied the IRS to resource allocation in full-duplex

cognitive systems. They enhanced the performance of the secondary networks and mitigated interference to primary users by a multi-parameter optimization scheme, including a phase shift matrix at the IRS. Dao and Sun [28] obtained the outage probabilities as exact and asymptotic closed-form expressions for evaluating IRS-supported multi-constraint two-way full-duplex underlay systems. Yuan and others [30] investigated multiple IRSs to a downlink multiple-input single-output cognitive radio network. They attempted to maximize the achievable rate of the secondary user under the constraints of total transmit power and interference temperature. Zhang and others [31] jointly optimized the transmit precoding at the secondary user and phase shifts at the IRS to minimize the total transmit power. However, non-convex optimization problems become more complex under intricate constraints and more computationally intensive with the phase shift matrix. The abovementioned works omitted short packet transmission and analytical studies of the system performance.

The aforementioned works indicate the necessity of IRS-assisted short packet communication in cognitive radio networks. In this paper, we propose and analyze short packet communication in an underlay cognitive radio network under multi-interference constraints of the primary receivers. Our network, called the SPC-UCR network, is assisted by a multiple-reconfigurable-reflector IRS in a scheme denoted as the IRS protocol. Short packets are sent in a single time slot (TS) and the IRS enhances the end-to-end signal-to-noise ratio (SNR) by adjusting its phases until the phases received at a secondary destination sum to zero. The transmit power of the secondary source is optimized to maximize the performance under all interference constraints without exceeding its maximum allowance. The system performance of the proposed IRS protocol is evaluated using the single-integral, infinity-sum, and asymptotic average BLERs.

1.2 | Contributions

Our main contributions are as follows: (1) we enhance the system performance of the SPC-UCR network with the proposed IRS protocol by installing a larger number of reconfigurable reflectors, setting a larger blocklength, sending fewer information bits, or reducing the number of allowed primary receivers; (2) we maximize the average BLER performance of the proposed IRS protocol by setting identical distances from the IRS to the secondary source and the secondary destination; (3) we show that the proposed IRS protocol always outperforms the corresponding underlay relaying protocols using two TSs to send short packets through a cooperative relay; and (4) we validate the theoretical analysis results (single-integral, infinite-sum, asymptotic and exact closed-form expressions) of the average BLERs in Monte Carlo simulations.

TABLE 1 Notation table

Notation	Meaning
$f_\Upsilon(\cdot)$	Probability density function (PDF) of a random variable Υ
$F_\Upsilon(\cdot)$	Cumulative distribution function (CDF) of a random variable Υ
$\Pr[\Xi]$	Probability operation of an event Ξ
$\mathrm{E}[\cdot]$	Expectation operator
$\mathrm{Var}[\cdot]$	Variance operator
$\binom{k}{M}$	Binomial coefficient, $\binom{k}{M} = \frac{M!}{k!(M-k)!}$
$\Gamma[x]$	Gamma function [32] (Equation 8.310)
$\gamma[x,y]$	Lower incomplete Gamma function [32] (Equation 8.350.1)
$\Gamma[x,y]$	Upper incomplete Gamma function [32] (Equation 8.350.2)
$\Upsilon \sim CN(0, N_0)$	Complex Gaussian random variable Υ with zero mean and variance N_0 [22]
$\|\|$	Magnitude
$\|\|^2$	Gain
$\mathrm{E}_y(x)$	Exponential integral function [33] (Equation 1), $\mathrm{E}_y(x) = \int\limits_1^\infty (e^{-xt}/t^y)\mathrm{d}t$
$Q(x)$	Gaussian Q-function [4], $Q(x) = \frac{1}{\sqrt{2\pi}}\int\limits_x^\infty e^{-y^2}/2\mathrm{d}y$

1.3 | Paper outline and notations

The remainder of this paper is organized into the following sections. Section 2 presents a system model of the IRS-supported underlay cognitive network. Section 3 analyzes the average BLERs of the proposed IRS protocol and the benchmark protocols. Section 4 presents the results and discussion and Section 5 summarizes our contributions.

Table 1 lists the notations used in this paper.

2 | SYSTEM MODEL

Figure 1 shows the system model with an IRS-supported underlay network. The secondary source (S) attempts to send information with σ bits to the secondary destination through an IRS with L reconfigurable reflectors, denoted as T_l, $l = \{1, 2, ..., L\}$. The secondary nodes S and D tolerate the interference constraints of M primary receivers PR_i, denoted as I_i, $i = \{1, 2, ..., M\}$; this operation is called the IRS protocol. The secondary source S, secondary destination D and M primary receivers are equipped in one antenna[1]. In Figure 1, (h_{ST_l}, d_{ST_l}), (h_{T_lD}, d_{T_lD}) and (h_{SP_i}, d_{SP_i}) denote the pairs of fading channel coefficients and normalized distances of links $S-T_l$, T_l-D and $S-PR_i$, respectively. It is assumed that (1) pairs (S, D) and (T_l, PR_i) are not directly linked because they are far apart, subjected to deep shadow fading and low reflecting power of the IRS, or the beam is formed only at D of the IRS [24]; (2) all primary receivers PR_i are distributed in a cluster and each T_l is close to others, so the normalized distances can be set as $d_{ST_l} = d_{ST}$, $d_{T_lD} = d_{TD}$ and $d_{SP_i} = d_{SP}$ [34, 35]; (3) all fading channel coefficients are complex normal random variables (RVs), that is, $h_{ST_l} = |h_{ST_l}| \; e^{j\varphi_{ST_l}} \sim CN(0, 1/\lambda_{ST})$, $h_{T_lD} = |h_{T_lD}|e^{j\varphi_{T_lD}} \sim CN(0, 1/\lambda_{TD})$ and $h_{SP_i} \sim CN(0, 1/\lambda_{SP})$, where the pairs $(|h_{ST_l}|, \varphi_{ST_l})$ and $(|h_{T_lD}|, \varphi_{T_lD})$ are the amplitude and phase values of channels h_{ST_l} and h_{T_lD}, respectively, $\lambda_\kappa = d_\kappa^\beta$, β is the path-loss exponent [22, 24, 26, 36], $\kappa \in \{ST, TD, SP\}$, and $j^2 = -1$. Consequently, $|h_{ST_l}|$ and $|h_{T_lD}|$ are independent RVs and follow the Rayleigh distribution with means given by $E[|h_{ST_l}|] = 1/2\sqrt{\pi/\lambda_{ST}}$, $E[|h_{T_lD}|] = \frac{1}{2}\sqrt{\pi/\lambda_{TD}}$ and variances given by $Var[|h_{ST_l}|] = (1 - \pi/4)/\lambda_{ST}$ and $Var[|h_{T_lD}|] = (1 - \pi/4)/\lambda_{TD}$, respectively [37] (eq. 6–70).

Under the operation conditions of the underlay cognitive radio network, the transmit power of the secondary source S (denoted by P_S) cannot exceed the maximum power (denoted by P_{max}); that is, $P_S \leq P_{max}$.
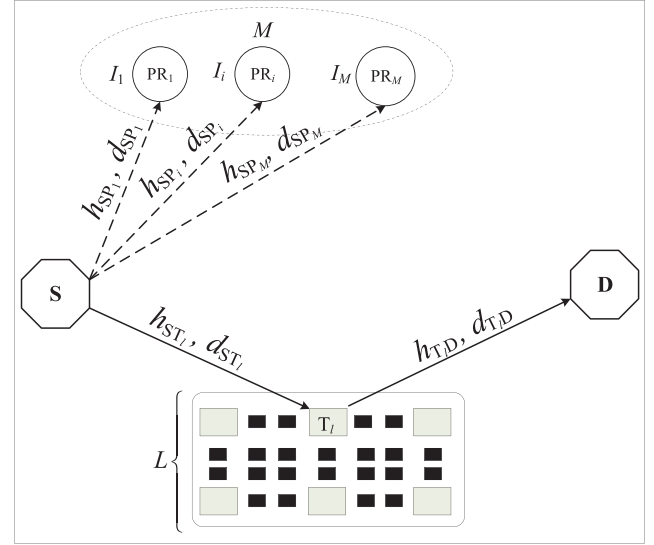

FIGURE 1 System model of an intelligent reflecting surface (IRS)-supported underlay cognitive network

All interference constraints of the primary network, including PR_i, $P_S \leq I_i/g_{SP_i}$ [21], must also be satisfied. Therefore, P_S is optimally set as $P_S = \min(P_{max}, I_1/g_{SP_1}, I_2/g_{SP_2}, ..., I_M/g_{SP_M})$ [38] where $g_{SP_i} = |h_{SP_i}|^2$ and $i = \{1, 2, ..., M\}$. According to previous works [34, 39], g_{SP_i} is an exponential RV with PDF and CDF given by $f_{g_{SP_i}}(x) = \lambda_{SP}e^{-\lambda_{SP}x}$ and $F_{g_{SP_i}}(x) = 1 - e^{-\lambda_{SP}x}$, respectively.

In the proposed IRS protocol, the secondary source S transmits a signal s with blocklength η to a secondary destination D through the IRS. The received signal at D is presented as

$$y_{IRS}^D = \sqrt{P_S} \left(\sum_{l=1}^{L} h_{ST_l} r_l h_{T_lD} \right) s + n_D, \qquad (1)$$

where r_l is the unit-adjusted response of the T_l, which can be expressed as $r_l = e^{j\varphi_l}$ with φ_l being the adjustable phase induced by T_l [22, 26], $n_D \sim CN(0, N_0)$ is additive Gaussian noise, and $E\{|s|^2\} = 1$.

The received end-to-end SNR at D, which decodes s, is obtained from (1) as

$$\gamma_{IRS}^D = \frac{\left| \sqrt{P_S}s \left(\sum_{l=1}^{L} h_{ST_l} r_l h_{T_lD} \right) \right|^2}{N_0}$$

$$= \frac{P_S \left| \left(\sum_{l=1}^{L} |h_{ST_l}|e^{j\varphi_{ST_l}} e^{j\varphi_l} |h_{T_lD}|e^{j\varphi_{T_lD}} \right) \right|^2}{N_0} \qquad (2)$$

$$= \frac{P_S \left(\sum_{l=1}^{L} |h_{ST_l}| \times |h_{T_lD}|e^{j(\varphi_l + \varphi_{ST_l} + \varphi_{T_lD})} \right)^2}{N_0}.$$

To maximize $\gamma_{\text{IRS}}^{\text{D}}$ in (2), the phases φ_l of the T_l are optimally selected as $\varphi_l = -\left(\varphi_{\text{ST}_l} + \varphi_{\text{T}_l\text{D}}\right)$ by varactor-tuned resonators. The phases of CSI h_{ST_l} and $h_{\text{T}_l\text{D}}$ are perfectly known [22,24–26,28]. The resonator can tune the phase shift φ_l by adjusting the bias voltage on its varactor [26]. The best end-to-end SNR in (2) is obtained as

$$\gamma_{\text{IRS}}^{\text{D}} = \frac{\left| \left(\sqrt{P_{\text{S}}} \displaystyle\sum_{l=1}^{L} |h_{\text{ST}_l}| \times |h_{\text{T}_l\text{D}}| \right) s \right|^2}{N_0}$$

$$= \frac{P_{\text{S}} \left(\displaystyle\sum_{l=1}^{L} |h_{\text{ST}_l}| \times |h_{\text{T}_l\text{D}}| \right)^2}{N_0}. \tag{3}$$

The instantaneous BLER of decoding s at D is expressed as [8]

$$\varepsilon^{\text{IRS}} \approx Q \left(\frac{C(\gamma_{\text{IRS}}^{\text{D}}) - \frac{\sigma}{\eta}}{\sqrt{V(\gamma_{\text{IRS}}^{\text{D}})/\eta}} \right), \tag{4}$$

where the functions $C(x)$ and $V(x)$ are respectively defined as $C(x) = \log_2(1+x)$ and $V(x) = \left(1 - (1/(1+x))^2\right)(\log_2 e)^2$, and $Q(x)$ is the Gaussian Q-function in López and others [4]; specifically, $Q(x) = (1/\sqrt{2\pi}) \int_x^\infty \exp(-y^2/2) dy$. The blocklength η of the short packet communications is considered in large-value cases ($\eta > 100$) to ensure a well-approximated operator [8].

For comparison purposes, we also consider short packet communication in underlay cognitive radio networks assisted by cooperative (DF or AF) relay without the IRS. Here, the operations with DF and AF cooperative relays are called the DF and AF protocols, respectively. The cooperative relay is located at the IRS. The end-to-end SNR at D, which decodes s, is expressed as [2, 17, 25]

$$\gamma_{\text{D}}^{\text{X}} = \begin{cases} \min(\gamma_{\text{SR}}, \gamma_{\text{RD}}), & \text{if } \text{X} = \text{DF} \\ \dfrac{\gamma_{\text{SR}}\gamma_{\text{RD}}}{\gamma_{\text{SR}} + \gamma_{\text{RD}} + 1}, & \text{if } \text{X} = \text{AF}, \end{cases} \tag{5}$$

where $\gamma_{\text{SR}} = P_{\text{S}}|h_{\text{SR}}|^2/N_0$ and $\gamma_{\text{RD}} = P_{\max}|h_{\text{RD}}|^2/N_0$; h_{SR} and h_{RD} denote the fading channel coefficients of the links from S to relay and from relay to D, respectively. They are respectively given by $h_{\text{SR}} \sim CN(0, 1/\lambda_{\text{ST}})$ and $h_{\text{RD}} \sim CN(0, 1/\lambda_{\text{TD}})$.

The instantaneous BLER of decoding s at D in the comparison protocols is computed as

$$\varepsilon^{\text{X}} \approx Q \left(\frac{C(\gamma_{\text{X}}^{\text{D}}) - \frac{\sigma}{\eta}}{\sqrt{V(\gamma_{\text{X}}^{\text{D}})/\eta}} \right), \tag{6}$$

where $\text{X} \in \{\text{DF, AF}\}$.

3 | AVERAGE BLER

To simplify the presentations, we place identical constraints on the tolerable interferences of all M primary receivers PR_i; that is, $I_1 = I_2 = \ldots = I_M = I$ [38]. In addition, we set the parameter groups as $\chi = P_{\max}/N_{\text{o}}$, $\psi = I/N_{\text{o}}$, and $\Theta = \sum_{l=1}^{L} |h_{\text{ST}_l}| \times |h_{\text{T}_l\text{D}}|$.

The average BLER of the SPC-UCR network is determined as [8, 11]

$$\overline{\varepsilon^{\text{X}}} = \text{E}\{\varepsilon^{\text{X}}\} \approx \text{E} \left\{ Q \left(\frac{C(\gamma_{\text{X}}^{\text{D}}) - \frac{\sigma}{\eta}}{\sqrt{V(\gamma_{\text{X}}^{\text{D}})/\eta}} \right) \right\}$$

$$= \int_0^\infty Q \left(\frac{C(\gamma_{\text{X}}^{\text{D}}) - \frac{\sigma}{\eta}}{\sqrt{V(\gamma_{\text{X}}^{\text{D}})/\eta}} \right) \times f_{\gamma_{\text{X}}^{\text{D}}}(x) dx \tag{7}$$

$$\approx \nu\sqrt{\eta} \int_{\rho_1}^{\rho_2} F_{\gamma_{\text{X}}^{\text{D}}}(x) dx,$$

where $f_{\gamma_{\text{X}}^{\text{D}}}(x)$ and $F_{\gamma_{\text{X}}^{\text{D}}}(x)$ are the PDF and CDF of the received SNR $\gamma_{\text{X}}^{\text{D}}$, respectively, for $\text{X} \in \{\text{IRS, DF, AF}\}$, $\nu = \left(2\pi\sqrt{2^{2\sigma/\eta} - 1}\right)^{-1}$, $\rho_1 = 2^{\sigma/\eta} - 1 - \left(2\nu\sqrt{\eta}\right)^{-1}$, and $\rho_2 = 2^{\sigma/\eta} - 1 + \left(2\nu\sqrt{\eta}\right)^{-1}$.

3.1 | The proposed IRS protocol

To analyze the average BLER of the SPC-UCR network with the proposed IRS protocol, we express the CDF $F_{\gamma_{\text{D}}^{\text{IRS}}}(x)$ as

$$F_{\gamma_{\text{D}}^{\text{IRS}}}(x) = \Pr\left[\gamma_{\text{D}}^{\text{IRS}} < x\right] = \Pr\left[\frac{P_{\text{S}}\Theta^2}{N_0} < x\right]$$

$$= \Pr\left[\frac{\Theta^2 \min\left(P_{\max}, I/g_{\text{SP}_1}, I/g_{\text{SP}_2}, \ldots, I/g_{\text{SP}_M}\right)}{N_0} < x\right] \tag{8}$$

$$= \Pr\left[\Theta^2 \min\left(\chi, \psi / \max_{i=1,2,\ldots,M}(g_{\text{SP}_i})\right) < x\right].$$

Setting $g_{\text{SP}_m} = \max_{i=1,2,\ldots,M}(g_{\text{SP}_i})$, where $m \in \{1, 2, \ldots, M\}$ in (8), we obtain

$$F_{\gamma_D^{IRS}}(x) = \Pr\left[\Theta^2 \min\left(\chi, \psi/g_{SP_m}\right) < x\right]$$
$$= \underbrace{\Pr\left[\left(\chi\Theta^2 < x\right) \cap \left(\chi \leq \psi/g_{SP_m}\right)\right]}_{A(x)}$$
$$+ \underbrace{\Pr\left[\left(\psi\Theta^2/g_{SP_m} < x\right) \cap \left(\chi > \psi/g_{SP_m}\right)\right]}_{B(x)}. \tag{9}$$

Remark 1. Note that $F_{\gamma_D^{IRS}}(x) \to \Pr\left[\Theta^2\chi < x\right]$ as $\psi \to +\infty$. This is the limiting condition of (9).

Before finding closed-form expressions of $A(x)$ and $B(x)$ in (9), we give the PDFs and CDFs of the RVs g_{SP_m} and Θ in the forms of Lemmas 1 and 2:

Lemma 1. The CDF and PDF of the RV g_{SP_m} are respectively obtained as

$$F_{g_{SP_m}}(x) \stackrel{(10a)}{=} \left(1 - e^{-\lambda_{SP}x}\right)^M$$
$$\stackrel{(10b)}{=} \sum_{i=0}^{M}\binom{i}{M}(-1)^i e^{-i\lambda_{SP}x}, \tag{10}$$

$$f_{g_{SP_m}}(x) \stackrel{(11a)}{=} M\lambda_{SP}e^{-\lambda_{SP}x}\left(1 - e^{-\lambda_{SP}x}\right)^{M-1}$$
$$\stackrel{(11b)}{=} \lambda_{SP}\sum_{i=1}^{M}\binom{i}{M}i(-1)^{i+1}e^{-i\lambda_{SP}x}. \tag{11}$$

The proof is given in Papoulis and Pillai [37] (Equations 7–14) and Son and others [39] (Equations 4 and 5).

Lemma 2. The PDF and CDF of the RV Θ are respectively found as

$$f_\Theta(x) = \frac{x^u e^{-x/v}}{v^{u+1}\Gamma[u+1]}, \tag{12}$$

$$F_\Theta(x) \stackrel{(13a)}{=} \frac{\gamma\left[u+1, \frac{x}{v}\right]}{\Gamma[u+1]} \stackrel{(13b)}{=} 1 - \frac{\Gamma\left[u+1, \frac{x}{v}\right]}{\Gamma[u+1]}, \tag{13}$$

where $\mu = L\pi/\left(4\sqrt{\lambda_{ST}\lambda_{TD}}\right), \vartheta = L(1-\pi^2/16)/(\lambda_{ST}\lambda_{TD})$, $u = \mu^2/\vartheta - 1$, and $v = \vartheta/\mu$. $\gamma[x,y], \Gamma[x,y]$, and $\Gamma[x]$ represent the lower incomplete Gamma function [32] (Equation 8.350.1), the upper incomplete Gamma function [32] (Equation 8.350.2), and the Gamma function [32] (Equation 8.310.1), respectively. They are related as $\gamma[x,y] + \Gamma[x,y] = \Gamma[x]$ [32] (Equation 8.356.3).

Proof. As demonstrated in previous works [28,34], the product term $|h_{ST_l}| \times |h_{T_lD}|$ in the RV Θ is a double Rayleigh distributed RV. From previous works [26,28], the PDF and CDF of Θ are obtained as (12) and (13), respectively, where $u = \mu^2/\vartheta - 1$ and $v = \vartheta/\mu$. First, μ can be expressed, manipulated and solved as

$$\mu = E[\Theta] = E\left[\sum_{l=1}^{L}|h_{ST_l}| \times |h_{T_lD}|\right]$$
$$= \sum_{l=1}^{L}\left(E[|h_{ST_l}|] \times E[|h_{T_lD}|]\right) \tag{14}$$
$$= \sum_{l=1}^{L}\left(\frac{1}{2}\sqrt{\frac{\pi}{\lambda_{ST}}}\frac{1}{2}\sqrt{\frac{\pi}{\lambda_{TD}}}\right) = \frac{L\pi}{4\sqrt{\lambda_{ST}\lambda_{TD}}}.$$

Next, the parameter ϑ is stated as

$$\vartheta = Var[\Theta] = E\left[\Theta^2\right] - (E[\Theta])^2$$
$$= E\left[\left(\sum_{l=1}^{L}|h_{ST_l}| \times |h_{T_lD}|\right)^2\right] - \mu^2$$
$$= \sum_{l=1}^{L}E\left[|h_{ST_l}|^2 \times |h_{T_lD}|^2\right] + L(L-1)$$
$$\times E[|h_{ST_\varpi}| \times |h_{T_\varpi D}| \times |h_{ST_\tau}| \times |h_{T_\tau D}|] - \mu^2$$
$$= \sum_{l=1}^{L}\left(E\left[|h_{ST_l}|^2\right] \times E\left[|h_{T_lD}|^2\right]\right) + L(L-1)$$
$$\times E[|h_{ST_\varpi}|] \times E[|h_{T_\varpi D}|] \times E[|h_{ST_\tau}|] \times E[|h_{T_\tau D}|] - \mu^2, \tag{15}$$

where $\varpi, \tau \in \{1, 2, ..., L\}$ and $\varpi \neq \tau$.

In (15), $|h_{ST_l}|^2$ and $|h_{T_lD}|^2$ are exponential RVs [34, 39], so $E[|h_{ST_l}|^2] = 1/\lambda_{ST}$ and $E[|h_{T_lD}|^2] = 1/\lambda_{TD}$. Substituting the mean of the Rayleigh distributions into (15), ϑ is finally solved as

$$\vartheta = \frac{L}{\lambda_{ST}\lambda_{TD}} + L(L-1)\left(\frac{1}{2}\sqrt{\frac{\pi}{\lambda_{ST}}}\right)^2\left(\frac{1}{2}\sqrt{\frac{\pi}{\lambda_{TD}}}\right)^2$$
$$- \left(\frac{L\pi}{4\sqrt{\lambda_{ST}\lambda_{TD}}}\right)^2 = \frac{L}{\lambda_{ST}\lambda_{TD}}\left(1 - \frac{\pi^2}{16}\right), \tag{16}$$

which completes the proof of Lemma 2.

The function $A(x)$ in (9) is equivalently expressed as

$$A(x) = \Pr\left[\left(\Theta^2 < x/\chi\right) \cap \left(g_{SP_m} \le \psi/\chi\right)\right]$$
$$= \Pr\left[\left(\Theta < \sqrt{x/\chi}\right) \cap \left(g_{SP_m} \le \psi/\chi\right)\right] \quad (17)$$
$$= F_\Theta\left(\sqrt{x/\chi}\right) \times F_{g_{SP_m}}\left(\psi/\chi\right).$$

Substituting the exponential representation of $F_{g_{SP_m}}(\psi/\chi)$ in (10a) and (13b) into (17), $A(x)$ is obtained as

$$A(x) = \left\{1 - \frac{\Gamma\left[u+1, \frac{\sqrt{x/\chi}}{v}\right]}{\Gamma[u+1]}\right\} \times \left(1 - e^{-\lambda_{SP}\psi/\chi}\right)^M. \quad (18)$$

Similarly, the function $B(x)$ in (9) becomes

$$B(x) = \Pr\left[\left(\Theta < \sqrt{xg_{SP_m}/\psi}\right) \cap \left(g_{SP_m} > \psi/\chi\right)\right]$$
$$= \int_{\psi/\chi}^{\infty} F_\Theta\left(\sqrt{xy/\psi}\right) \times f_{g_{SP_m}}(y)\mathrm{d}y. \quad (19)$$

From (7) and (9), the average BLER of the SPC-UCR network with the proposed IRS protocol is computed as

$$\overline{\varepsilon^{IRS}} \approx v\sqrt{\eta} \int_{\rho_1}^{\rho_2} (A(x) + B(x))\mathrm{d}x$$
$$= v\sqrt{\eta}\left(\underbrace{\int_{\rho_1}^{\rho_2} A(x)\mathrm{d}x}_{\mathfrak{I}_1} + \underbrace{\int_{\rho_1}^{\rho_2} B(x)\mathrm{d}x}_{\mathfrak{I}_2}\right). \quad (20)$$

Substituting $A(x)$ in (18) into the integral $\mathfrak{I}_1$ in (20), we obtain

$$\mathfrak{I}_1 = \int_{\rho_1}^{\rho_2}\left(1 - \frac{\Gamma\left[u+1, \frac{\sqrt{x/\chi}}{v}\right]}{\Gamma[u+1]}\right) \times \left(1 - e^{-\lambda_{SP}\psi/\chi}\right)^M \mathrm{d}x$$
$$= \left(1 - e^{-\lambda_{SP}\psi/\chi}\right)^M\left(\rho_2 - \rho_1 - \frac{1}{\Gamma[u+1]}\int_{\rho_1}^{\rho_2}\Gamma\left[u+1, \frac{\sqrt{x/\chi}}{v}\right]\mathrm{d}x\right). \quad (21)$$

In terms of the variable $y = \sqrt{x}$, (21) is rewritten as

$$\mathfrak{I}_1 = \left(1 - e^{-\lambda_{SP}\psi/\chi}\right)^M\left(\rho_2 - \rho_1 - \frac{2}{\Gamma[u+1]}\int_{\sqrt{\rho_1}}^{\sqrt{\rho_2}} y\Gamma\left[u+1, \frac{y}{v\sqrt{\chi}}\right]\mathrm{d}y\right)$$
$$= \left(1 - e^{-\lambda_{SP}\psi/\chi}\right)^M\left(\rho_2 - \rho_1 - \frac{1}{\Gamma[u+1]}\left(\Delta_1\left(\sqrt{\rho_2}\right) - \Delta_1\left(\sqrt{\rho_1}\right)\right)\right), \quad (22)$$

where the function $\Delta_1(x)$ is clearly defined as

$$\Delta_1(x) = x^2\left(\begin{array}{c}\Gamma\left[u+1, \frac{x}{v\sqrt{\chi}}\right] - \left(x/(v\sqrt{\chi})\right)^u e^{-x/(v\sqrt{\chi})} \\ -(u+2)\left(x/(v\sqrt{\chi})\right)^u \mathrm{E}_{-(u+1)}\left(x/(v\sqrt{\chi})\right)\end{array}\right). \quad (23)$$

In (23), $\mathrm{E}_y(x)$ is the exponential integral function $\mathrm{E}_y(x) = \int_1^\infty (e^{-xt}/t^y)\mathrm{d}t$ (Equation (1) in Alkheir and Ibnkahla [33]).

Substituting (22) into (20), $\overline{\varepsilon^{IRS}}$ is clarified as follows:

$$\overline{\varepsilon^{IRS}} \approx v\sqrt{\eta}\left(\left(1 - e^{-\lambda_{SP}\psi/\chi}\right)^M \right.$$
$$\left. \times \left(\rho_2 - \rho_1 - \frac{1}{\Gamma[u+1]}\left(\Delta_1\left(\sqrt{\rho_2}\right) - \Delta_1\left(\sqrt{\rho_1}\right)\right)\right) + \mathfrak{I}_2\right). \quad (24)$$

To express $\mathfrak{I}_2$ in (24), we substitute $B(x)$ given by (19) into the integral $\mathfrak{I}_2$ in (20):

$$\mathfrak{I}_2 = \int_{\rho_1}^{\rho_2}\int_{\psi/\chi}^{\infty} F_\Theta\left(\sqrt{xy/\psi}\right) \times f_{g_{SP_m}}(y)\mathrm{d}y\mathrm{d}x$$
$$= \int_{\psi/\chi}^{\infty}\left(\int_{\rho_1}^{\rho_2} F_\Theta\left(\sqrt{xy/\psi}\right)\mathrm{d}x\right) \times f_{g_{SP_m}}(y)\mathrm{d}y. \quad (25)$$

Lemma 3. $\mathfrak{I}_2$ can be expressed in single integral as follows:

$$\mathfrak{I}_2 = (\rho_2 - \rho_1)\left(1 - \left(1 - e^{-\lambda_{SP}\psi/\chi}\right)^M\right)$$
$$- \frac{M\lambda_{SP}}{\Gamma[u+1]}\int_{\psi/\chi}^{\infty}(\Delta_2(\rho_2, y) - \Delta_2(\rho_1, y))e^{-\lambda_{SP}y}\left(1 - e^{-\lambda_{SP}y}\right)^{M-1}\mathrm{d}y, \quad (26)$$

where the function $\Delta_2(x, y)$ is presented in closed form as follows:

$$\Delta_2(x,y) = \Gamma\left[u+1, \frac{\sqrt{xy/\psi}}{v}\right]\left(x - \frac{v^2\psi}{y}(u+1)(u+2)\right)$$
$$- \frac{v^2\psi}{y}\left(\frac{\sqrt{xy/\psi}}{v}\right)^{u+1} e^{-\frac{\sqrt{xy/\psi}}{v}}\left(u+2+\frac{\sqrt{xy/\psi}}{v}\right). \tag{27}$$

Proof. Substituting (13b) into (25) gives the following results:

$$\mathfrak{I}_2 = \int_{\psi/\chi}^{\infty}\left(\int_{\rho_1}^{\rho_2}\left(1 - \frac{\Gamma\left[u+1, \frac{\sqrt{xy/\psi}}{v}\right]}{\Gamma[u+1]}\right)dx\right) \times f_{g_{SP_m}}(y)dy$$

$$= \int_{\psi/\chi}^{\infty}\int_{\rho_1}^{\rho_2} f_{g_{SP_m}}(y)dxdy - \int_{\psi/\chi}^{\infty}\left(\int_{\rho_1}^{\rho_2}\frac{\Gamma\left[u+1, \frac{\sqrt{xy/\psi}}{v}\right]}{\Gamma[u+1]}dx\right)f_{g_{SP_m}}(y)dy$$

$$= (\rho_2 - \rho_1)\left(1 - F_{g_{SP_m}}(\psi/\chi)\right)$$
$$- \frac{1}{\Gamma[u+1]}\int_{\psi/\chi}^{\infty}\left(\int_{\rho_1}^{\rho_2}\Gamma\left(u+1, \frac{\sqrt{xy/\psi}}{v}\right)dx\right) \times f_{g_{SP_m}}(y)dy$$

$$= (\rho_2 - \rho_1)\left(1 - F_{g_{SP_m}}(\psi/\chi)\right) - \frac{1}{\Gamma[u+1]}$$
$$\times \int_{\psi/\chi}^{\infty}\left(\begin{array}{c}\Gamma\left[u+1, \frac{\sqrt{\rho_2 y/\psi}}{v}\right]\rho_2 - \Gamma\left[u+1, \frac{\sqrt{\rho_1 y/\psi}}{v}\right]\rho_1 \\ - \frac{v^2\psi}{y}\left(\Gamma\left[u+3, \frac{\sqrt{\rho_2 y/\psi}}{v}\right] - \Gamma\left[u+3, \frac{\sqrt{\rho_1 y/\psi}}{v}\right]\rho_1\right)\end{array}\right)f_{g_{SP_m}}(y)dy. \tag{28}$$

Lemma 3 is solved using Equation (8.256.2) in Gradshteyn and others [32] followed by the CDF and PDF of the RV g_{SP_m} (10a and 11a).

Lemma 4. The integral $\mathfrak{I}_2$ over $N \to +\infty$ can be presented as an infinite sum:

$$\mathfrak{I}_2 = \frac{2}{\Gamma(u+1)}\sum_{i=1}^{M}\binom{i}{M}\sum_{n=0}^{N}\frac{(-1)^{i+n+1}\left(\rho_2^{\frac{u+n+3}{2}} - \rho_1^{\frac{u+n+3}{2}}\right)}{(i\lambda_{SP}\psi v^2)^{\frac{u+n+1}{2}}n!(u+n+1)(u+n+3)}$$
$$\times\left(\Gamma\left[\frac{u+n+3}{2}\right] + \Gamma\left[\frac{u+n+3}{2}, \frac{i\lambda_{SP}\psi}{\chi}\right] - \left(\frac{u+n+1}{2}\right)\Gamma\left[\frac{u+n+1}{2}\right]\right). \tag{29}$$

Proof. Substituting (11b) and (13a) into (19) and using the infinite-sum expression $\gamma\left[u+1, \sqrt{xy/\psi}/v\right] = \sum_{n=0}^{N}(-1)^n$

$\left(\sqrt{xy/\psi}/v\right)^{u+n+1}/n!(u+n+1)$ in Gradshteyn and others [32] (eq. 8.354), where $N \to +\infty$, we get

$$B(x) = \frac{\lambda_{SP}}{\Gamma[u+1]}\sum_{i=1}^{M}\binom{i}{M}i(-1)^{i+1}$$
$$\times \sum_{n=0}^{N}\frac{(-1)^n}{n!(u+n+1)}\left(\frac{\sqrt{x/\psi}}{v}\right)^{u+n+1}\int_{\psi/\chi}^{\infty}y^{(u+n+1)/2}e^{-i\lambda_{SP}y}dy$$
$$= \frac{1}{\Gamma[u+1]}\sum_{i=1}^{M}\binom{i}{M}\sum_{n=0}^{N}\frac{(-1)^{i+n+1}\left(\sqrt{x/\psi}/v\right)^{(u+n+1)}}{n!(u+n+1)}(i\lambda_{SP})^{-(u+n+1)/2}$$
$$\times\left(\Gamma\left[\frac{u+n+3}{2}\right] + \Gamma\left[\frac{u+n+3}{2}, \frac{i\lambda_{SP}\psi}{\chi}\right] - \left(\frac{u+n+1}{2}\right)\Gamma\left[\frac{u+n+1}{2}\right]\right). \tag{30}$$

Having obtained $B(x)$, the integral $\mathfrak{I}_2$ in (20) is solved as

$$\mathfrak{I}_2 = \frac{1}{\Gamma[u+1]}\sum_{i=1}^{M}\binom{i}{M}\sum_{n=0}^{N}\frac{(-1)^{i+n+1}(i\lambda_{SP})^{-(u+n+1)/2}}{n!(u+n+1)(\psi v^2)^{\frac{u+n+1}{2}}}$$
$$\times\left(\begin{array}{c}\Gamma\left[\frac{u+n+3}{2}\right] + \Gamma\left[\frac{u+n+3}{2}, \frac{i\lambda_{SP}\psi}{\chi}\right] \\ - \left(\frac{u+n+1}{2}\right)\times\Gamma\left[\frac{u+n+1}{2}\right]\end{array}\right)\int_{\rho_1}^{\rho_2}x^{(u+n+1)/2}dx. \tag{31}$$

The integral in (31) is easily solved to prove Lemma 4.

Theorem 1. *The average BLER of the SPC-UCR network with the proposed IRS protocol ($\overline{\varepsilon^{\mathrm{IRS}}}$) is obtained as an exact single-integral form and an infinite-sum form. The expression is given by (32) at the top of the following page.*

Proof. Theorem 1 can be proven using Lemmas 3 and 4 for the average BLER of the proposed IRS protocol ($\overline{\varepsilon^{IRS}}$), which is given by (24).

To gain additional insights, we evaluate the average BLER of the SPC-UCR network with the proposed IRS protocol from $\psi \to +\infty$. The presentation is given as Remark 2.

Remark 2. As $\psi \to +\infty$, the average BLER of the SPC-UCR network with the proposed IRS protocol asymptotically

3.2 | The benchmark protocols

The CDF $F_{\gamma_{\mathrm{D}}^{\mathrm{DF}}}(x)$ of the SPC-UCR network with the DF protocol is expressed as

$$
\overline{\varepsilon^{\mathrm{IRS}}} \stackrel{(32a)}{\approx} v\sqrt{\eta}\left(\rho_2 - \rho_1 - \frac{1}{\Gamma[u+1]}\left(\left(1 - e^{-\lambda_{\mathrm{SP}}\psi/\chi}\right)^M \left(\Delta_1\left(\sqrt{\rho_2}\right) - \Delta_1\left(\sqrt{\rho_1}\right)\right) + M\lambda_{\mathrm{SP}}\int_{\psi/\chi}^{\infty}(\Delta_2(\rho_2, y) - \Delta_2(\rho_1, y))e^{-\lambda_{\mathrm{SP}}y}\left(1 - e^{-\lambda_{\mathrm{SP}}y}\right)^{M-1}\mathrm{d}y\right)\right)
$$

$$
\stackrel{(32b)}{=} v\sqrt{\eta}\left(\begin{array}{l}\left(1 - e^{-\lambda_{\mathrm{SP}}\psi/\chi}\right)^M\left(\rho_2 - \rho_1 - \frac{1}{\Gamma[u+1]}\left(\Delta_1\left(\sqrt{\rho_2}\right) - \Delta_1\left(\sqrt{\rho_1}\right)\right)\right) + \frac{2}{\Gamma(u+1)}\sum_{i=1}^{M}(iM)\sum_{n=0}^{N}\frac{(-1)^{i+n+1}\left(\rho_2^{\frac{u+n+3}{2}} - \rho_1^{\frac{u+n+3}{2}}\right)}{(i\lambda_{\mathrm{SP}}\psi v^2)^{\frac{u+n+1}{2}}n!(u+n+1)(u+n+3)}\\ \times\left(\Gamma\left[\frac{u+n+3}{2}\right] + \Gamma\left[\frac{u+n+3}{2}, \frac{i\lambda_{\mathrm{SP}}\psi}{\chi}\right] - \left(\frac{u+n+1}{2}\right)\Gamma\left[\frac{u+n+1}{2}\right]\right)\end{array}\right).
$$

$$(32)$$

becomes

$$
\overline{\varepsilon^{\mathrm{IRS}}}_{\psi\to+\infty} \approx v\sqrt{\eta}\int_{\rho_1}^{\rho_2}\Pr\left[\Theta^2\chi < x\right]\mathrm{d}x
$$

$$
= v\sqrt{\eta}\int_{\rho_1}^{\rho_2}F_\Theta\left(\sqrt{x/\chi}\right)\mathrm{d}x
$$

$$
= v\sqrt{\eta}\int_{\rho_1}^{\rho_2}\left(1 - \frac{\Gamma\left[u+1, \frac{\sqrt{x/\chi}}{v}\right]}{\Gamma[u+1]}\right)\mathrm{d}x
$$

$$
= v\sqrt{\eta}\left(\rho_2 - \rho_1 - \frac{\Delta_1\left(\sqrt{\rho_2}\right) - \Delta_1\left(\sqrt{\rho_1}\right)}{\Gamma[u+1]}\right).
$$

$$(33)$$

The accuracy of the infinite sum form in (32b) can be evaluated by the following error metric [4]:

$$
\xi = \frac{\left|\overline{\varepsilon^{\mathrm{IRS}}}_{\mathrm{ex}} - \overline{\varepsilon^{\mathrm{IRS}}}_{\mathrm{ap}}\right|}{\overline{\varepsilon^{\mathrm{IRS}}}_{\mathrm{ex}}},
$$

$$(34)$$

where $\overline{\varepsilon^{\mathrm{IRS}}}_{\mathrm{ex}}$ and $\overline{\varepsilon^{\mathrm{IRS}}}_{\mathrm{ap}}$ are the exact and approximated average BLERs obtained by (32a) and (32b), respectively.

$$
\begin{aligned}
F_{\gamma_{\mathrm{D}}^{\mathrm{DF}}}(x) &= \Pr\left[\gamma_{\mathrm{D}}^{\mathrm{DF}} < x\right] = \Pr[\min(\gamma_{\mathrm{SR}}, \gamma_{\mathrm{RD}}) < x]\\
&= \Pr\left[\min\left(\frac{P_{\mathrm{S}}|h_{\mathrm{SR}}|^2}{N_0}, \frac{P_{\max}|h_{\mathrm{RD}}|^2}{N_0}\right) < x\right]\\
&= \Pr\left[\min\left(\frac{\min(P_{\max}, I/g_{\mathrm{SP}_1}, I/g_{\mathrm{SP}_2}, ..., I/g_{\mathrm{SP}_M})g_{\mathrm{SR}}}{N_0}, \chi g_{\mathrm{RD}}\right) < x\right]\\
&= \Pr[\min(\chi g_{\mathrm{SR}}, \psi g_{\mathrm{SR}}/g_{\mathrm{SP}m}, \chi g_{\mathrm{RD}}) < x],
\end{aligned}
$$

$$(35)$$

where the exponentially distributed RVs are denoted as $g_{\mathrm{SR}} \triangleq |h_{\mathrm{SR}}|^2$ and $g_{\mathrm{RD}} \triangleq |h_{\mathrm{RD}}|^2$, respectively, and the PDF and CDF of g_κ are given by $f_{g_\kappa}(x) = \lambda_\kappa e^{-\lambda_\kappa x}$ and $F_{g_\kappa}(x) = 1 - e^{-\lambda_\kappa x}$, respectively, $\kappa \in \{\mathrm{SR}, \mathrm{RD}\}$, $\lambda_{\mathrm{SR}} = \lambda_{\mathrm{ST}}$, $\lambda_{\mathrm{RD}} = \lambda_{\mathrm{TD}}$.

Equation (35) can be rearranged as

$$
\begin{aligned}
F_{\gamma_{\mathrm{D}}^{\mathrm{DF}}}(x) &= 1 - \Pr[\min(\chi g_{\mathrm{SR}}, \psi g_{\mathrm{SR}}/g_{\mathrm{SP}m}, \chi g_{\mathrm{RD}}) \geq x]\\
&= 1 - \Pr[(\chi g_{\mathrm{SR}} \geq x) \cap (\psi g_{\mathrm{SR}}/g_{\mathrm{SP}m} \geq x) \cap (\chi g_{\mathrm{RD}} \geq x)]\\
&= 1 - \Pr[\chi g_{\mathrm{RD}} \geq x] \times \Pr[(\chi g_{\mathrm{SR}} \geq x) \cap (\psi g_{\mathrm{SR}}/g_{\mathrm{SP}m} \geq x)]\\
&= 1 - \Pr\left[g_{\mathrm{RD}} \geq \frac{x}{\chi}\right] \times \Pr\left[\left(g_{\mathrm{SR}} \geq \frac{x}{\chi}\right) \cap \left(g_{\mathrm{SP}m} \leq \frac{\psi g_{\mathrm{SR}}}{x}\right)\right]\\
&= 1 - \left(1 - F_{g_{\mathrm{RD}}}\left(\frac{x}{\chi}\right)\right) \times \int_{x/\chi}^{\infty} f_{g_{\mathrm{SR}}}(y) \times F_{g_{\mathrm{SP}m}}\left(\frac{\psi y}{x}\right)\mathrm{d}y\\
&= 1 - e^{-\lambda_{\mathrm{RD}}x/\chi} \times \int_{x/\chi}^{\infty} f_{g_{\mathrm{SR}}}(y) \times F_{g_{\mathrm{SP}m}}\left(\frac{\psi y}{x}\right)\mathrm{d}y.
\end{aligned}
$$

$$(36)$$

Remark 3. From (35) and (36), the asymptotic CDF $F_{\gamma_D^{DF}}(x)$ as $\psi \to +\infty$ is approximated as

Remark 4. As $\psi \to +\infty$, the average BLER of the SPC-UCR network with the DF protocol is asymptotically obtained as follows:

$$
\begin{aligned}
\overline{\varepsilon^{DF}} &\approx v\sqrt{\eta} \int_{\rho_1}^{\rho_2} \left(1 - \lambda_{SR} x e^{-x(\lambda_{SR}+\lambda_{RD})/\chi} \sum_{i=0}^{M} \binom{i}{M} (-1)^i \frac{e^{-i\lambda_{SP}\psi/\chi}}{\lambda_{SR}x + i\lambda_{SP}\psi} \right) dx \\
&= v\sqrt{\eta} \left(\rho_2 - \rho_1 - \sum_{i=0}^{M} \binom{i}{M} (-1)^i e^{-i\lambda_{SP}\psi/\chi} \int_{\rho_1}^{\rho_2} \frac{\lambda_{SR} x e^{-x(\lambda_{SR}+\lambda_{RD})/\chi}}{\lambda_{SR}x + i\lambda_{SP}\psi} dx \right) \\
&= v\sqrt{\eta} \left(\rho_2 - \rho_1 - \sum_{i=0}^{M} \binom{i}{M} (-1)^i e^{-i\lambda_{SP}\psi/\chi} \times \left(\frac{\chi}{\lambda_{SR}+\lambda_{RD}} \left(e^{-\rho_1(\lambda_{SR}+\lambda_{RD})/\chi} - e^{-\rho_2(\lambda_{SR}+\lambda_{RD})/\chi} \right) - \frac{i\lambda_{SP}\psi e^{i\lambda_{SP}\psi(\lambda_{SR}+\lambda_{RD})/(\chi\lambda_{SR})}}{\lambda_{SR}} \right. \right. \\
&\quad \left. \left. \times \left(\Gamma\left[0, \left(\frac{\lambda_{SR}+\lambda_{RD}}{\chi}\right)\left(\rho_1 + \frac{i\lambda_{SP}\psi}{\lambda_{SR}}\right) \right] - \Gamma\left[0, \left(\frac{\lambda_{SR}+\lambda_{RD}}{\chi}\right)\left(\rho_2 + \frac{i\lambda_{SP}\psi}{\lambda_{SR}}\right) \right] \right) \right) \right).
\end{aligned}
$$
(39)

$$
\begin{aligned}
F_{\gamma_D^{DF}}(x) &\approx \Pr[\min(\chi g_{SR}, \chi g_{RD}) < x] \\
&= 1 - \Pr[(\chi g_{SR} \geq x) \cap (\chi g_{RD} \geq x)] \\
&= 1 - \Pr\left[\left(g_{SR} \geq \frac{x}{\chi} \right) \right] \times \Pr\left[g_{RD} \geq \frac{x}{\chi} \right] \\
&= 1 - \left(1 - F_{g_{SR}}\left(\frac{x}{\chi}\right) \right) \times \left(1 - F_{g_{RD}}\left(\frac{x}{\chi}\right) \right) \\
&= 1 - e^{-x(\lambda_{SR}+\lambda_{RD})/\chi}.
\end{aligned}
$$
(37)

Substituting (10b) and $f_{g_{SR}}(y) = \lambda_{SR} e^{-\lambda_{SR} y}$ into (36), we obtain

$$
\begin{aligned}
&F_{\gamma_D^{DF}}(x) \\
&= 1 - e^{-\lambda_{RD}x/\chi} \times \int_{x/\chi}^{\infty} \lambda_{SR} e^{-\lambda_{SR} y} \times \sum_{i=0}^{M} \binom{i}{M} (-1)^i e^{-i\lambda_{SP}\psi y/x} dy \\
&= 1 - \lambda_{SR} e^{-\lambda_{RD}x/\chi} \sum_{i=0}^{M} \binom{i}{M} (-1)^i \int_{x/\chi}^{\infty} e^{-y(\lambda_{SR}+i\lambda_{SP}\psi/x)} dy \\
&= 1 - \lambda_{SR} x e^{-x(\lambda_{SR}+\lambda_{RD})/\chi} \sum_{i=0}^{M} \binom{i}{M} (-1)^i \frac{e^{-i\lambda_{SP}\psi/\chi}}{\lambda_{SR}x + i\lambda_{SP}\psi}.
\end{aligned}
$$
(38)

Substituting (38) into (7), we obtain the average BLER of the SPC-UCR network with the DF protocol. The formula (39) is given at the top of the next page.

$$
\begin{aligned}
&\overline{\varepsilon_{\psi \to +\infty}^{DF}} \\
&\approx v\sqrt{\eta} \int_{\rho_1}^{\rho_2} \left(1 - e^{-x(\lambda_{SR}+\lambda_{RD})/\chi} \right) dx \\
&= v\sqrt{\eta} \left(\rho_2 - \rho_1 + \frac{\chi\left(e^{-\rho_2(\lambda_{SR}+\lambda_{RD})/\chi} - e^{-\rho_1(\lambda_{SR}+\lambda_{RD})/\chi} \right)}{\lambda_{SR}+\lambda_{RD}} \right).
\end{aligned}
$$
(40)

In the SPC-UCR network with the AF protocol, the CDF $F_{\gamma_D^{AF}}(x)$ is similarly obtained as

$$
\begin{aligned}
F_{\gamma_D^{AF}}(x) &= \Pr[\gamma_D^{AF} < x] = \Pr\left[\frac{\gamma_{SR}\gamma_{RD}}{\gamma_{SR}+\gamma_{RD}+1} < x \right] \\
&= \Pr\left[\frac{\frac{P_S|h_{SR}|^2}{N_0} \frac{P_{max}|h_{RD}|^2}{N_0}}{\frac{P_S|h_{SR}|^2}{N_0} + \frac{P_{max}|h_{RD}|^2}{N_0} + 1} < x \right] \\
&= \Pr\left[\frac{\chi g_{RD} \min(\chi g_{SR}, \psi g_{SR}/g_{SPm})}{\chi g_{RD} + \min(\chi g_{SR}, \psi g_{SR}/g_{SPm}) + 1} < x \right].
\end{aligned}
$$
(41)

Remark 5. To the authors knowledge, the CDF $F_{\gamma_D^{AF}}(x)$ given by (41) does not admit a closed-form mathematical expression. Referring to previous works [40–42], the end-to-end SNR at D in the AF protocol is approximated by its upper bound as

$$\gamma_{\mathrm{D}}^{\mathrm{AF}} = \frac{\gamma_{\mathrm{SR}}\gamma_{\mathrm{RD}}}{\gamma_{\mathrm{SR}}+\gamma_{\mathrm{RD}}+1} < \min(\gamma_{\mathrm{SR}},\gamma_{\mathrm{RD}}) = \gamma_{\mathrm{D}}^{\mathrm{DF}}. \qquad (42)$$

Hence, the average BLER of the SPC-UCR network with the AF protocol is lower-bounded by the $\overline{\varepsilon^{\mathrm{DF}}}$ given by (39).

Remark 6. Equations (33) and (40) show that $\overline{\varepsilon^{\mathrm{IRS}}}$ and $\overline{\varepsilon^{\mathrm{DF}}}$ at high ψ values (as $\psi \to +\infty$) are independent of ψ, meaning that the diversity gains of both the IRS and DF protocols approach 0. As proof of this remark, the diversity gains of these protocols are respectively given by

$$\begin{aligned} \mathrm{DG}^{\mathrm{IRS}} &= -\lim_{\psi\to+\infty} \frac{\log_{10}\overline{\varepsilon^{\mathrm{IRS}}}}{\log_{10}\psi} \\ &= -\lim_{\psi\to+\infty} \frac{\log_{10}\overline{\varepsilon^{\mathrm{IRS}}_{\psi\to+\infty}}}{\log_{10}\psi} = 0, \end{aligned} \qquad (43)$$

$$\begin{aligned} \mathrm{DG}^{\mathrm{DF}} &= -\lim_{\psi\to+\infty} \frac{\log_{10}\overline{\varepsilon^{\mathrm{DF}}}}{\log_{10}\psi} \\ &= -\lim_{\psi\to+\infty} \frac{\log_{10}\overline{\varepsilon^{\mathrm{DF}}_{\psi\to+\infty}}}{\log_{10}\psi} = 0. \end{aligned} \qquad (44)$$

4 | NUMERICAL RESULTS AND DISCUSSION

This section presents and discusses the analysis and simulation results in the two-dimensional plane. The coordinates of the S, D, and IRS nodes in the proposed IRS protocol (or cooperative relay in the comparison protocols DF and AF) were $(0,0)$, $(1,0)$, and $(x_{\mathrm{X}},y_{\mathrm{X}})$, respectively, and the cluster with M primary receivers PR_i was located at $(x_{\mathrm{PR}},y_{\mathrm{PR}})$. Here, $\mathrm{X} \in \{\mathrm{IRS},\mathrm{DF},\mathrm{AF}\}$, $0 < x_{\mathrm{X}} < 1$, and $i = \{1,2,...,M\}$. The normalized distances were determined as $d_{SX} = \sqrt{x_{\mathrm{X}}^2 + y_{\mathrm{X}}^2}$, $d_{XD} = \sqrt{(1-x_{\mathrm{X}})^2 + y_{\mathrm{X}}^2}$ and $d_{SP} = \sqrt{x_{\mathrm{PR}}^2 + y_{\mathrm{PR}}^2}$. The path-loss exponent was fixed at $\beta = 3$. The simulations were executed by the Monte Carlo method and the analytical results were calculated using the theoretical expressions.

We first discuss the accuracy of the error metric expressed as an infinite sum. Figure 2 plots the error metric ξ in (34) versus number of summed terms (N). The parameters were fixed at $\psi = 5$ (dB), $\chi = -5$ (dB), $M = 3$, $\sigma = 256$ (bits), $\eta = 512$ (bits), $x_{\mathrm{PR}} = 0$, $y_{\mathrm{PR}} = 0.5$, $x_{\mathrm{IRS}} = 0.5$, $y_{\mathrm{IRS}} = -0.5$, and $L = \in \{2,3,4,5\}$. As
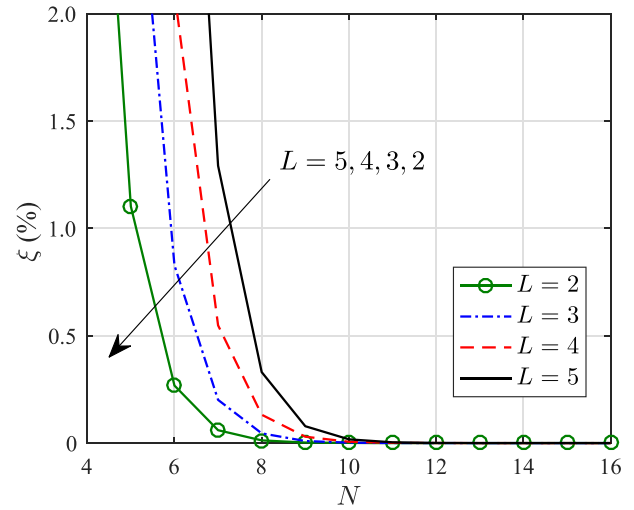

FIGURE 2 Error metric ξ versus number of terms in the infinite sum (N): $\psi = 5$ (dB), $\chi = -5$ (dB), $M = 3$, $\sigma = 256$ (bits), $\eta = 512$ (bits), $x_{\mathrm{PR}} = 0$, $y_{\mathrm{PR}} = 0.5$, $x_{\mathrm{IRS}} = 0.5$, $y_{\mathrm{IRS}} = -0.5$, and $L \in \{2,3,4,5\}$
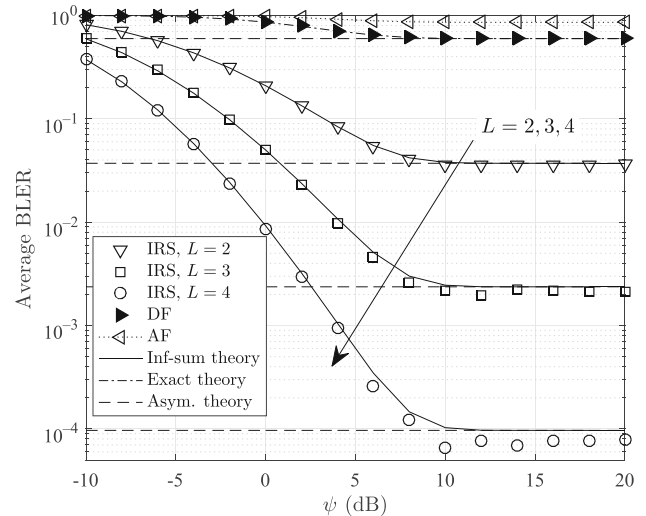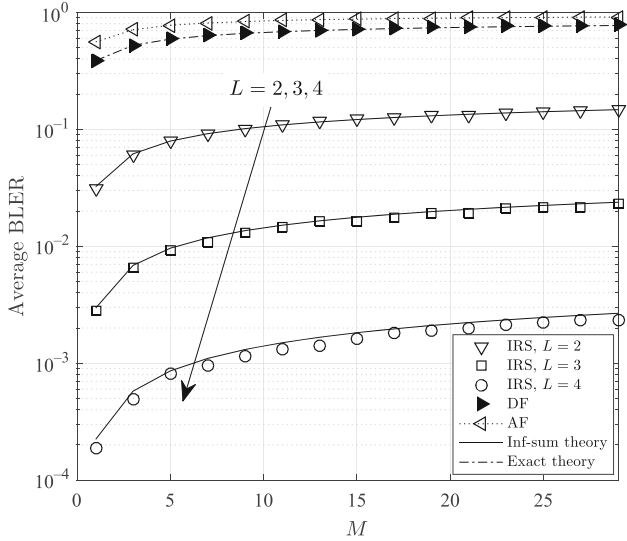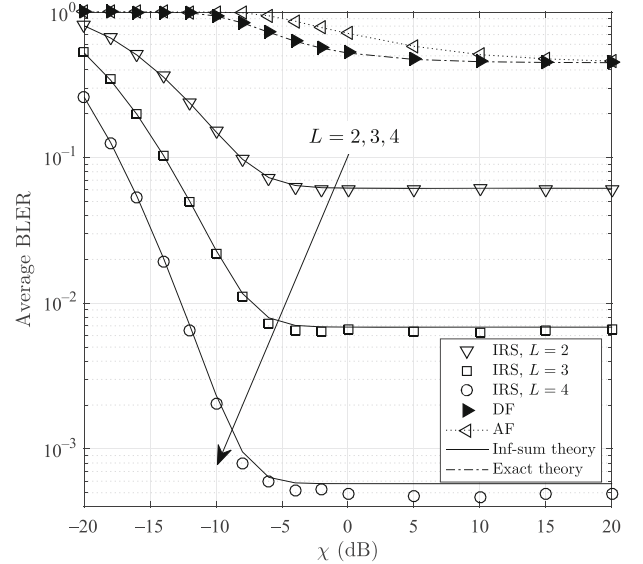

FIGURE 3 Average block error rate (BLER) versus ψ (dB) for $\chi = -5$ (dB), $\sigma = 256$ (bits), $\eta = 512$ (bits), $x_{\mathrm{PR}} = 0$, $y_{\mathrm{PR}} = 0.5$, $x_{\mathrm{IRS}} = 0.5$, $y_{\mathrm{IRS}} = -0.5$, $M = 3$, and $L \in \{2,3,4\}$

the number of reconfigurable reflectors L decreased, fewer terms in the infinity sum (N) (32b) were required to achieve a good approximation. Regardless of L, the error metric ξ quickly converged to a very small value (e.g. $\xi < 0.4\%$ at $N > 8$). Hence, the infinite sum of the average BLER of the proposed IRS protocol (32b) well approximates the exact form (32a), even when truncated to a limited number of elements.

TABLE 2 N versus L and ψ (dB)

$L \searrow \psi$	−10	−8	−6	−4	−2	0	2	4	6	8	10	12	14	16	18	20
2	54	40	30	23	18	14	11	9	7	6	5	3	1	1	1	1
3	60	45	34	26	20	16	13	10	8	6	5	3	1	1	1	1
4	67	50	38	29	23	18	14	11	9	7	5	3	1	1	1	1

FIGURE 4 Average block error rate (BLER) versus M for $\psi = 5$ (dB), $\chi = 0$ (dB), $\sigma = 256$ (bits), $\eta = 512$ (bits), $x_{PR} = 0$, $y_{PR} = 0.5$, $x_X = 0.5$, $y_X = -0.5$, and $L \in \{2, 3, 4\}$

FIGURE 5 Average block error rate (BLER) versus χ (dB) for $\psi = 5$ (dB), $\sigma = 256$ (bits), $\eta = 512$ (bits), $x_{PR} = 0$, $y_{PR} = 0.5$, $x_X = 0.5$, $y_X = -0.5$, $M = 3$ and $L \in \{2, 3, 4\}$

Figure 3 plots the average BLERs of the proposed IRS protocol and the benchmark protocols (DF and AF protocols) versus ψ (dB). The parameters were fixed to $\chi = -5$ (dB), $\sigma = 256$ (bits), $\eta = 512$ (bits), $x_{PR} = 0$, $y_{PR} = 0.5$, $x_{IRS} = 0.5$, $y_{IRS} = -0.5$, and $M = 3$. The number of reconfigurable reflectors (L) was varied as $L \in \{2, 3, 4\}$. In Figure 3 and the following figures, the markers, solid lines, dotted-dashed lines, and dashed lines denote the simulated, infinite-sum, exact closed-form, and asymptotic solutions of the protocols, respectively. In the simulated results of the SPC-UCR network with the AF protocol, the lower-bound average BLERs of the AF protocol matched the exact theory of the DF protocol. As the number of terms in (32b) decreased in the theoretical analysis of infinite sum, the difference between two consecutive average BLERs converged to 10^{-5}, meaning that $\left| \overline{\varepsilon^{IRS}}(N) - \overline{\varepsilon^{IRS}}(N+1) \right| < 10^{-5}$. Table 2 lists the ψ values in Figure 3 for different numbers of terms (N) in the infinite sum (columns) versus number of reconfigurable reflectors (rows). Reducing N reduced the complexity of the average BLER

analysis in the proposed IRS protocol. Observing Figure 3, we observe that under all protocols, the BLER performance of the SPC-UCR network improved after providing higher interference-constraint parameters ψ (defined as I/N_o) and by reducing the number of primary receivers. The performance of the proposed IRS protocol was also rapidly enhanced by increasing the number of reconfigurable reflectors. Third, the proposed IRS protocol always outperformed the DF and AF relaying protocols. Fourth, the average BLERs of the IRS, DF and AF protocols moved toward the error floor as ψ increased, that is, at $\psi > 10$ (dB). Finally, the infinite-sum and closed-form theory analyses of the average BLERs were consistent with Monte Carlo simulations and the asymptotic theory was reasonable from $\psi \to +\infty$. These discoveries can be explained as follows. As ψ increases, the transmitted power of the secondary source can be increased by optimizing the power allocation, which promotes large end-to-end SNRs. In particular, when the transmit powers are optimized, the interference constraints of the primary receivers exert a trivial effect at

large ψ values, so the secondary source can transmit only at the constant maximum power P_{max} to reach the BLER floor. More importantly, as shown in (3), increasing the number of reconfigurable reflectors improved the end-to-end SNR in the proposed IRS protocol.

Figure 4 shows the effect of varying the number of primary receivers (M) on the average BLER of the SPC-UCR network under the three protocols. The BLER performances under all protocols declined as the number
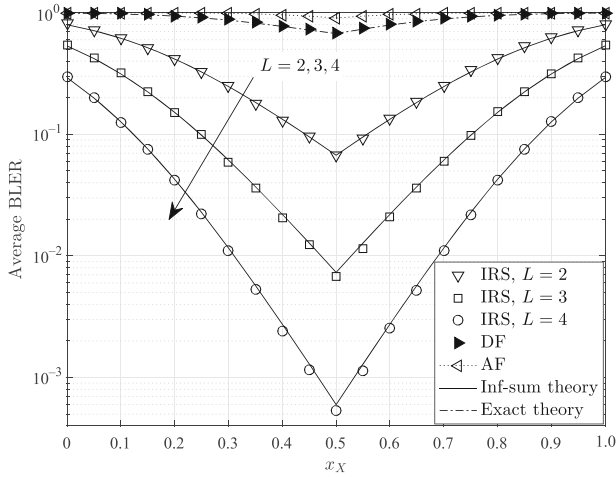
of primary receivers increased because the received end-to-end SNRs given by (3) and (5) are weakened by interferences from multiple primary receivers. Furthermore, the maximum number of terms (N) required to create the theoretical infinite sum was 11, indicating that the proposed IRS protocol can reduce the complexity of the mathematical calculation.

Figure 5 presents the average BLER of the proposed IRS and benchmark protocols versus χ (dB). The parameters were set to $\psi = 5$ (dB), $\sigma = 256$ (bits), $\eta = 512$ (bits), $x_{PR} = 0, y_{PR} = 0.5, x_X = 0.5, y_X = -0.5, M = 3$, and $L \in \{2, 3, 4\}$. The BLERs in all protocols decreased with increasing χ. Under the proposed protocol, χ saturated at around -6 dB. When χ is large, the transmitted power of the secondary source P_S is affected only by the fixed interference constraint ($\psi = 5$ (dB)) and the constant-mean channel gains. Therefore, both the average BLERs given by (7) and the average end-to-end SNRs given by (3) and (5) converged to constant values with increasing χ. This result confirms that the proposed IRS protocol outperforms the DF and AF protocols when the number of reconfigurable reflectors is large.

Figure 6 plots the BLER performances of the considered protocols versus locations of the reconfigurable reflectors or cooperative relays (denoted as x_X) when $\psi = 5$ (dB), $\chi = -5$ (dB), $\sigma = 256$ (bits), $\eta = 512$ (bits), $M = 3$ and $L \in \{2, 3, 4\}$. The node locations are shown in Figure 7. The PRs were fixed at (0, 0.5) and the reconfigurable reflectors or cooperative relays were moved from point A to C through B along the lines $y_X = x_X - 1$ if $0 \le x_X \le 0.5$ and $y_X = -x_X$ if $0.5 < x_X \le 1$. As shown in Figure 6, all protocols achieved their best performances

FIGURE 6 Average block error rate (BLER) versus x_X for $\psi = 5$ (dB), $\chi = -5$ (dB), $\sigma = 256$ (bits), $\eta = 512$ (bits), $M = 3$, $L \in \{2, 3, 4\}$ and $y_X = \{x_X - 1, 0 \le x_X \le 0.5 - x_X, 0.5 < x_X \le 1$
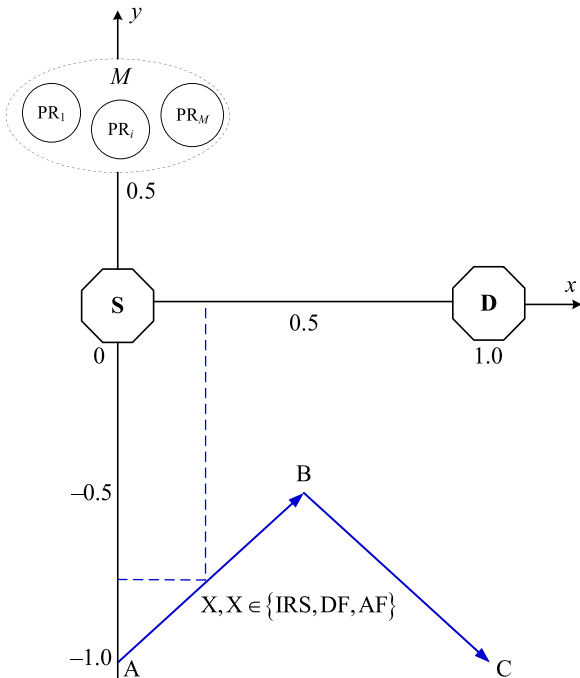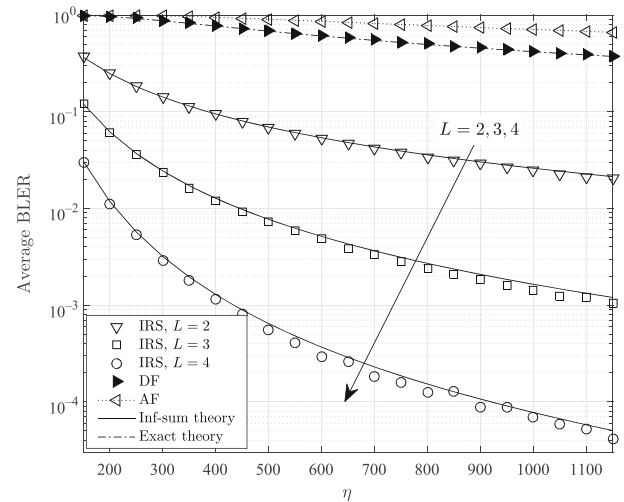

FIGURE 7 The location of the nodes in Figure 6

FIGURE 8 Average block error rate (BLER) versus η for $\psi = 5$ (dB), $\chi = -5$ (dB), $\sigma = 256$ (bits), $x_{PR} = 0, y_{PR} = 0.5, x_X = 0.5$, $y_X = -0.5, M = 3$, and $L \in \{2, 3, 4\}$
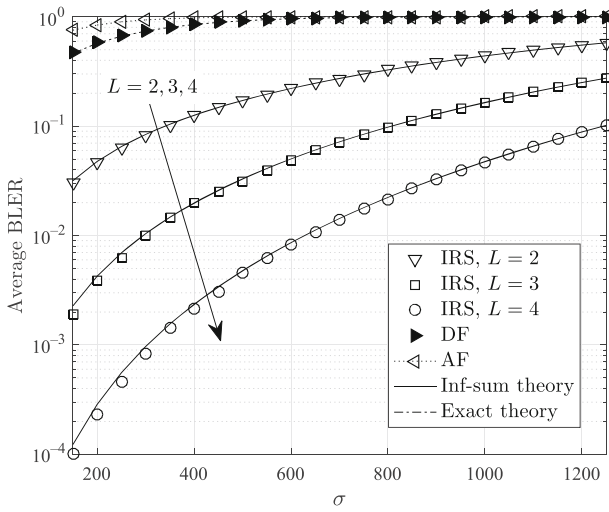
FIGURE 9 Average block error rate (BLER) versus σ for $\psi = 5$ (dB), $\chi = -5$ (dB), $\eta = 512$ (bits), $x_{PR} = 0$, $y_{PR} = 0.5$, $x_X = 0.5$, $y_X = -0.5$, $M = 3$ and $L \in \{2, 3, 4\}$

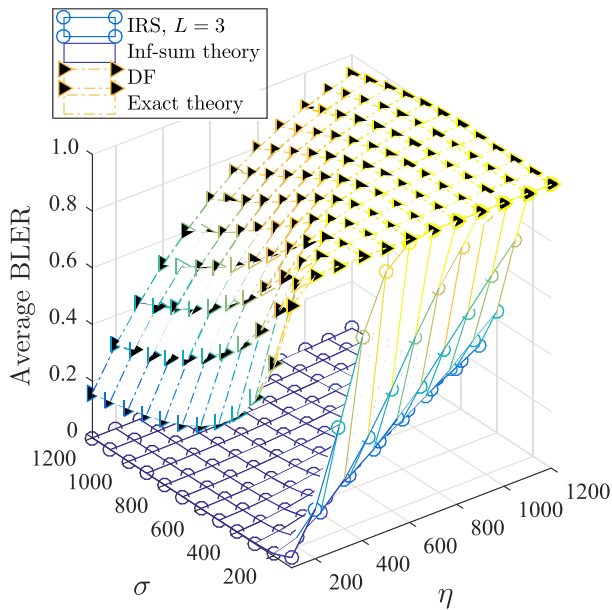**FIGURE 10** Average block error rate (BLER) versus η and σ for $\psi = 5$ (dB), $\chi = -5$ (dB), $x_{PR} = 0$, $y_{PR} = 0.5$, $x_X = 0.5$, $y_X = -0.5$, and $L = M = 3$

at $x_X = 0.5$ (and by inference, at $y_X = -0.5$), corresponding to identical distances from the reconfigurable reflectors (cooperative relay) to the secondary source and destination (i.e., $d_{ST} = d_{TD}$).

Next, the average BLERs of the IRS, DF and AF protocols were evaluated as functions of blocklength η. Figures 8 and 9 plot the results for different numbers of information bits ($\sigma = 256$ and 512 bits, respectively). The

remaining parameters were set as $\psi = 5$ (dB), $\chi = -5$ (dB), $x_{PR} = 0$, $y_{PR} = 0.5$, $x_X = 0.5$, $y_X = -0.5$, $M = 3$, and $L \in \{2, 3, 4\}$. The performance was improved by setting a larger blocklength, sending fewer information bits, and installing more reconfigurable reflectors.

Figure 10 summarizes the average BLERs of the IRS and DF protocols as functions of two variables, namely, η and σ, in three-dimensional coordinates. The other parameter values were set to $\psi = 5$ (dB), $\chi = -5$ (dB), $x_{PR} = 0$, $y_{PR} = 0.5$, $x_X = 0.5$, $y_X = -0.5$, and $L = M = 3$ while η and σ were varied from 100 to 1200 bits. The AF protocol is omitted from this figure to clarify the display. Figures 3–6 and 8 and 9 have already confirmed that the AF protocol is less efficient than the DF protocol. The BLER in both the IRS and DF protocols was minimized at the smallest η and the largest σ (Figure 10), that is, $\eta = 100$ bits and $\sigma = 1200$ bits. The results of Figure 10 confirm the accuracy of Figures 8 and 9 and provide a visual guide for optimizing the blocklength and number of information bits at a given average BLER.

5 | CONCLUSIONS

We proposed short packet transmission for an underlay cognitive radio network assisted by a multiple-reconfigurable-reflector IRS. The proposed IRS protocol can operate in a single TS under multi-interference constraints of the primary receivers. The IRS enhances the end-to-end SNR by adjusting its phases until the received cumulative phases at the secondary destination sum to zero. The transmitted power of the secondary source is optimized to satisfy all interference constraints and maximize the system performance within the limits of the maximum transmit power. The system performance of the proposed IRS protocol was evaluated by computing the single-integral, infinite-sum, and asymptotic average BLERs. As demonstrated in the simulation and analysis results, the performance of the IRS protocol can be improved by (1) installing a larger number of reconfigurable reflectors; (2) setting a larger blocklength; (3) sending fewer information bits; (4) reducing the number of allowed primary receivers. The proposed IRS protocol outperformed the benchmark DF and AF protocols (underlay relaying protocols without the IRS), which use two TSs to transmit short packets through a cooperative relay. The proposed IRS protocol and both benchmark protocols achieved their best performances when the IRS or cooperative relay was equidistant between the secondary source and secondary destination. Finally, the theoretical analysis results (single-integral, infinite-sum, asymptotic, and closed forms) of the average BLERs were confirmed by Monte Carlo simulations.

CONFLICT OF INTEREST
The authors declare that there are no conflicts of interest.

ORCID
Pham Ngoc Son https://orcid.org/0000-0002-9698-4221
Tran Trung Duy https://orcid.org/0000-0002-3947-2174

REFERENCES
1. H. Chen, R. Abbas, P. Cheng, M. Shirvanimoghaddam, W. Hardjawana, W. Bao, Y. Li, and B. Vucetic, *Ultra-reliable low latency cellular networks: use cases, challenges and approaches*, IEEE Commun. Mag. **56** (2018), no. 12, 119–125.

2. Y. Gu, H. Chen, Y. Li, L. Song, and B. Vucetic, *Short-packet two-way amplify-and-forward relaying*, IEEE Signal Process. Lett. **2** (2018), no. 7, 263–267.

3. Y. Gu, H. Chen, Y. Li, and B. Vucetic, *Ultra-reliable short-packet communications: half-duplex or full-duplex relaying?* IEEE Wireless Commun. Lett. **7** (2018), no. 3, 348–351.

4. O. L. A. López, E. M. G. Fernández, R. D. Souza, and H. Alves, *Ultra-reliable cooperative short-packet communications with wireless energy transfer*, IEEE Sensors J. **18** (2018), no. 5, 2161–2177.

5. P. Nouri, H. Alves, and M. Latva-aho, *Performance analysis of ultra-reliable short message decode and forward relaying protocols*, EURASIP J. Wirel. Commun. Netw. **2018** (2018), 1–14.

6. X. Huang and N. Yang, *On the block error performance of short-packet non-orthogonal multiple access systems*, (Proceedings of the ieee International Conference on Communications, Shanghai, China), 2019, pp. 1–7.

7. X. Lai, T. Wu, Q. Zhang, and J. Qin, *Average secure bler analysis of noma downlink short-packet communication systems in flat rayleigh fading channels*, IEEE Trans. Wirel. Commun. **20** (2021), no. 5, 2948–2960.

8. X. Lai, Q. Zhang, and J. Qin, *Cooperative noma short-packet communications in flat rayleigh fading channels*, IEEE Trans. Veh. Technol. **68** (2019), no. 6, 6182–6186.

9. D. Marasinghe, N. Rajatheva, and M. Latva-Aho, *Block error performance of NOMA with harq-cc in finite blocklength*, (Proceedings of the ieee International Conference on Communications Workshops, Dublin, Ireland), 2020, pp. 1–6.

10. Y. Yu, H. Chen, Y. Li, Z. Ding, and B. Vucetic, *On the performance of non-orthogonal multiple access in short-packet communications*, IEEE Commun. Lett. **22** (2018), no. 3, 590–593.

11. J. Zheng, Q. Zhang, and J. Qin, *Average block error rate of downlink noma short-packet communication systems in nakagami- m fading channels*, IEEE Commun. Lett. **23** (2019), no. 10, 1712–1716.

12. C. Li, N. Yang, and S. Yan, *Optimal transmission of short-packet communications in multiple-input single-output systems*, IEEE Trans. Veh. Technol. **68** (2019), no. 7, 7199–7203.

13. D.-D. Tran, S. K. Sharma, S. Chatzinotas, I. Woungang, and B. E. Ottersten, *Short-packet communications for mimo noma systems over nakagami-m fading: BLER and minimum block-length analysis*, IEEE Trans. Veh. Technol. **70** (2021), no. 4, 3583–3598.

14. Y. Chen, Z. Xiang, X. Qiao, T. Zhang, and J. Zhang, *Secure short-packet communications in cognitive internet of things*, (Proceedings of the 2020 ieee 3rd International Conference on Electronics and Communication Engineering (icece), Xi'an, China), 2020, pp. 31–36.

15. Y. Chen, T. Zhang, Y. Zhang, B. Yu, and Y. Cai, *Relay-assisted secure short-packet communications in cognitive internet of things*, (Proceedings of the 2021 IEEE International Conference on Communications workshops, Montreal, Canada), 2021, pp. 1–6.

16. Y. Chen, Y. Zhang, B. Yu, T. Zhang, and Y. Cai, *Relay-assisted secure short-packet transmission in cognitive IoT with spectrum sensing*, China Commun. **18** (2021), no. 12, 37–50.

17. C. D. Ho, T. V. Nguyen, T. Huynh-The, T. T. Nguyen, D. B. D. Costa, and B. An, *Short-packet communications in wireless-powered cognitive iot networks: performance analysis and deep learning evaluation*, IEEE Trans. Veh. Technol. **70** (2021), no. 3, 2894–2899.

18. H. Hu, Y. Huang, G. Cheng, Q. Kang, H. Zhang, and Y. Pan, *Optimization of energy efficiency in uav-enabled cognitive IoT with short packet communication*, IEEE Sensors J. **22** (2021), 12357–12368. https://doi.org/10.1109/JSEN.2021.3130581

19. T. H. Vu, T. V. Nguyen, T. T. Nguyen, and S. Kim, *Performance analysis and deep learning design of wireless powered cognitive NOMA IoT short-packet communications with imperfect csi and sic*, IEEE Internet Things J. **9** (2022), no.13, 10464–10479. https://doi.org/10.1109/JIOT.2021.3121421

20. A. Goldsmith, S. A. Jafar, I. Maric, and S. Srinivasa, *Breaking spectrum gridlock with cognitive radios: an information theoretic perspective*, Proc. IEEE **97** (2009), no. 5, 894–914.

21. T. Manimekalai, S. R. Joan, and T. Laxmikandan, *Throughput maximization for underlay cr multicarrier noma network with cooperative communication*, ETRI J. **42** (2020), no. 6, 846–858.

22. S. Atapattu, R. Fan, P. Dharmawansa, G. Wang, J. Evans, and T. A. Tsiftsis, *Reconfigurable intelligent surface assisted two-way communications: Performance analysis and optimization*, IEEE Trans. Commun. **68** (2020), no. 10, 6552–6567.

23. Q. Wu and R. Zhang, *Intelligent reflecting surface enhanced wireless network via joint active and passive beamforming*, IEEE Trans. Wirel. Commun. **18** (2019), no. 11, 5394–5409.

24. L. Yang, Y. Yang, D. B. D. Costa, and I. Trigui, *Outage probability and capacity scaling law of multiple ris-aided networks*, IEEE Wirel. Commun. Lett. **10** (2021), no. 2, 256–260.

25. E. Björnson, Özdogan Ö., and E. G. Larsson, *Intelligent reflecting surface versus decode-and-forward: How large surfaces are needed to beat relaying?*, IEEE Wireless Commun. Lett. **9** (2020), no. 2, 244–248.

26. A. A. Boulogeorgos and A. Alexiou, *Performance analysis of reconfigurable intelligent surface-assisted wireless systems and comparison with relaying*, IEEE Access **8** (2020), 94463–94483.

27. M. D. Renzo, K. Ntontin, J. Song, F. H. Danufane, X. Qian, F. Lazarakis, J. De Rosny, D. T. Phan-Huy, O. Simeone, R. Zhang, and M. Debbah, *Reconfigurable intelligent surfaces vs. relaying: differences, similarities, and performance comparison*, IEEE Open J. Commun. Soc. **1** (2020), 798–807.

28. T. T. T. Dao and P. N. Son, *Multi-constraint two-way underlay cognitive network using reconfigurable intelligent surface*, Wireless Netw. **28** (2022), 2017–2030. https://doi.org/10.1007/s11276-022-02959-1

29. D. Xu, X. Yu, Y. Sun, D. W. K. Ng, and R. Schober, *Resource allocation for irs-assisted full-duplex cognitive radio systems*, IEEE Trans. Commun. **68** (2020), no. 12, 7376–7394.

30. J. Yuan, Y. C. Liang, J. Joung, G. Feng, and E. G. Larsson, *Intelligent reflecting surface-assisted cognitive radio system*, IEEE Trans. Commun. **69** (2021), no. 1, 675–687.

31. L. Zhang, C. Pan, Y. Wang, H. Ren, and K. Wang, *Robust beamforming design for intelligent reflecting surface aided cognitive radio systems with imperfect cascaded CSI*, IEEE Trans. Cogn. Commun. Netw. **8** (2022), no. 1, 186–201.

32. R. I. Gradshteyn, I. S. Jeffrey, and A. D. Zwillinger, *Table of Integral, Series and Products*, 7th ed., Elsevier, Amsterdam, 2007.

33. A. A. Alkheir and M. Ibnkahla, *An accurate approximation of the exponential integral function using a sum of exponentials*, IEEE Commun. Lett. **17** (2013), no. 7, 1364–1367.

34. T. T. Duy, G. C. Alexandropoulos, V. T. Tung, V. N. Son, and T. Q. Duong, *Outage performance of cognitive cooperative networks with relay selection over double-rayleigh fading channels*, IET Commun. **10** (2016), no. 1, 57–64.

35. K. Tourki, K. A. Qaraqe, and M. Alouini, *Outage analysis for underlay cognitive networks using incremental regenerative relaying*, IEEE Trans. Veh. Technol. **62** (2013), no. 2, 721–734.

36. D. Kudathanthirige, D. Gunasinghe, and G. Amarasuriya, *Performance analysis of intelligent reflective surfaces for wireless communication*, (Proceedings of the ieee International Conference on Communications, Dublin, Ireland), 2020, pp. 1–6.

37. A. Papoulis and S. U. Pillai, *Probability, Random Variables and Stochastic Processes*, 2nd ed., McGraw-Hill, New York, 2002.

38. Y. Liu, Z. Ding, M. Elkashlan, and J. Yuan, *Nonorthogonal multiple access in large-scale underlay cognitive radio networks*, IEEE Trans. Veh. Technol. **65** (2016), no. 12, 10152–10157.

39. P. N. Son, T. T. Duy, and K. Ho-Van, *Sic-coding schemes for underlay two-way relaying cognitive networks*, Wirel. Commun. Mob. Comput. **2020** (2020), 1–17.

40. Z. Bai, J. Jia, C. Wang, and D. Yuan, *Performance analysis of snr-based incremental hybrid decode-amplify-forward cooperative relaying protocol*, IEEE Trans. Commun. **63** (2015), no. 6, 2094–2106.

41. S. Ikki and M. H. Ahmed, *Performance analysis of cooperative diversity wireless networks over nakagami-m fading channel*, IEEE Commun. Lett. **11** (2007), no. 4, 334–336.

42. T. Wang, A. Cano, G. B. Giannakis, and J. N. Laneman, *High-performance cooperative demodulation with decode-and-forward relays*, IEEE Trans. Commun. **55** (2007), no. 7, 1427–1438.

AUTHOR BIOGRAPHIES

Pham Ngoc Son received the BE degree (2005) and M. Eng. degree (2009) in Electronics and Telecommunications Engineering from the Post and Telecommunication Institute of Technology, Ho Chi Minh City and Ho Chi Minh City University of Technology, Vietnam, respectively. In 2015, he received the PhD degree in Electrical Engineering from University of Ulsan, South Korea. He is currently a Lecturer in the Faculty of Electrical and Electronics Engineering of Ho Chi Minh City University of Technology and Education. His major research interests are cooperative communication, cognitive radio, physical layer security, energy harvesting, nonorthogonal multiple access, intelligent reflecting surfaces, and short packet communications.

Tran Trung Duy received the PhD degree (2013) in electrical engineering from University of Ulsan, South Korea. From 2013 to the present, he joined the Posts and Telecommunications Institute of Technology (PTIT), Ho Chi Minh City campus. From 2017, he served as an associate editor of Transactions on Industrial Networks and Intelligent Systems. From 2021, he served as an associate editor of Hindawi Wireless Communications and Mobile Computing and Frontiers in Communications and Networks. His major research interests are cooperative communications, cooperative multi-hop, cognitive radio, physical-layer security, energy harvesting, hardware impairments, and Fountain codes.

Pham Viet Tuan received the BE degree (2005) and ME degree (2011) in Electronics and Telecommunications Engineering from Ho Chi Minh City University of Technology, Vietnam, and the PhD degree (2018) in Electrical and Computer Engineering from University of Ulsan, South Korea. He was a Postdoctoral Researcher at the Multimedia Communications System Laboratory, University of Ulsan, South Korea (2019). His research interests include optimization, machine learning, SWIPT MIMO systems, and intelligent reflecting surfaces.

Tan-Phuoc Huynh was born in 1979 in Di An City, Binh Duong Province. He received the PhD degree in Communication Technology from Technical University of Ostrava, Czech Republic. He is currently Head of Department of Computer Networks and Data Communications at the School of Computing and Information Technology, Eastern International University, Binh Duong City. His major research interests are wireless communications in 5G, non-orthogonal multiple access, energy harvesting, the performance of cognitive radio, network security, network programming, and Linux/Windows server operating system administration.